ADVANCED FUNCTIONAL MATERIALS

Supporting Information

for

Advanced Functional Materials, adfm.200600566

Supporting Information

One-Dimensional Tellurium Nanostructures: Photothermally Assisted Morphology-Controlled Synthesis and Applications in Preparing Functional Nanomaterials **

Bin Zhang, Weiyi Hou, Xingchen Ye, Shengquan Fu, and Yi Xie*

Department of Nanomaterials and Nanochemistry, Hefei National Laboratory for Physical Sciences at Microscale, University of Science and Technology of China, Hefei, Anhui 230026 (P. R. China)

E-mail: yxie@ustc.edu.cn

S1 SEM image of the as-prepared Te nanowires obtained in this visible-light assisted approach.

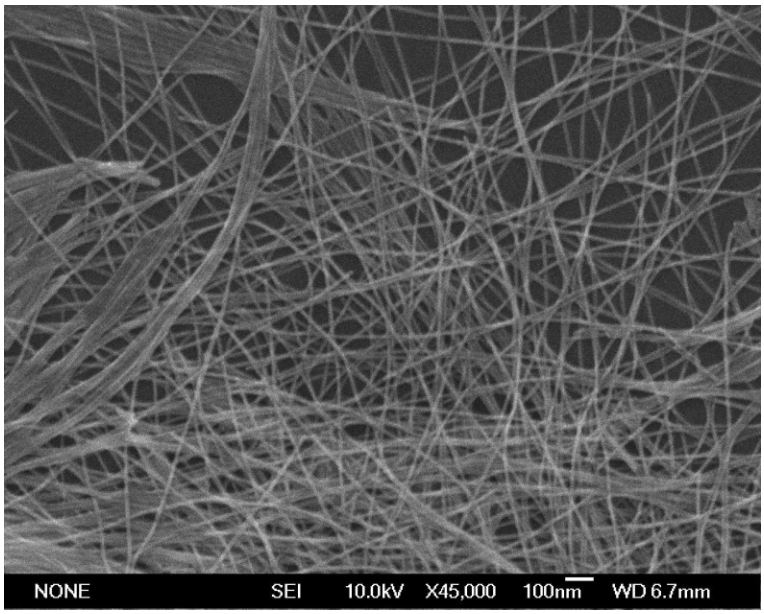

Figure S1. FESEM image of the as-prepared tellurium nanowires using the visible-light assisted method, revealing the large-scale preparation of uniform Te nanowires with ca. 12 nm in diameter and several microns in length. The samples was prepared in the presence of in the presence of 0.09 g H_2TeO_3, 0.05 g PVP, 1 mL $N_2H_4 \cdot H_2O$ and 100 mL H_2O

S2 TEM image of the as-prepared Te nanotubes obtained in this visible-light assisted approach.

Figure S2. TEM image of the as-prepared Te nanotubes prepared in the presence of 0.09 g H_2TeO_3, 0.15 g PVP, 1 mL $N_2H_4{\cdot}H_2O$ and 100 mL H_2O by using the visible-light assisted method, revealing the large-scale preparation of Te nanotubes. The inset is the higher magnification TEM image, further confirming the tubular shape of the Te products.

S3 TEM image of the as-prepared Te nanoparticles and nanoparticle-joint quai-1D nanostructures obtained in this visible-light assisted approach.

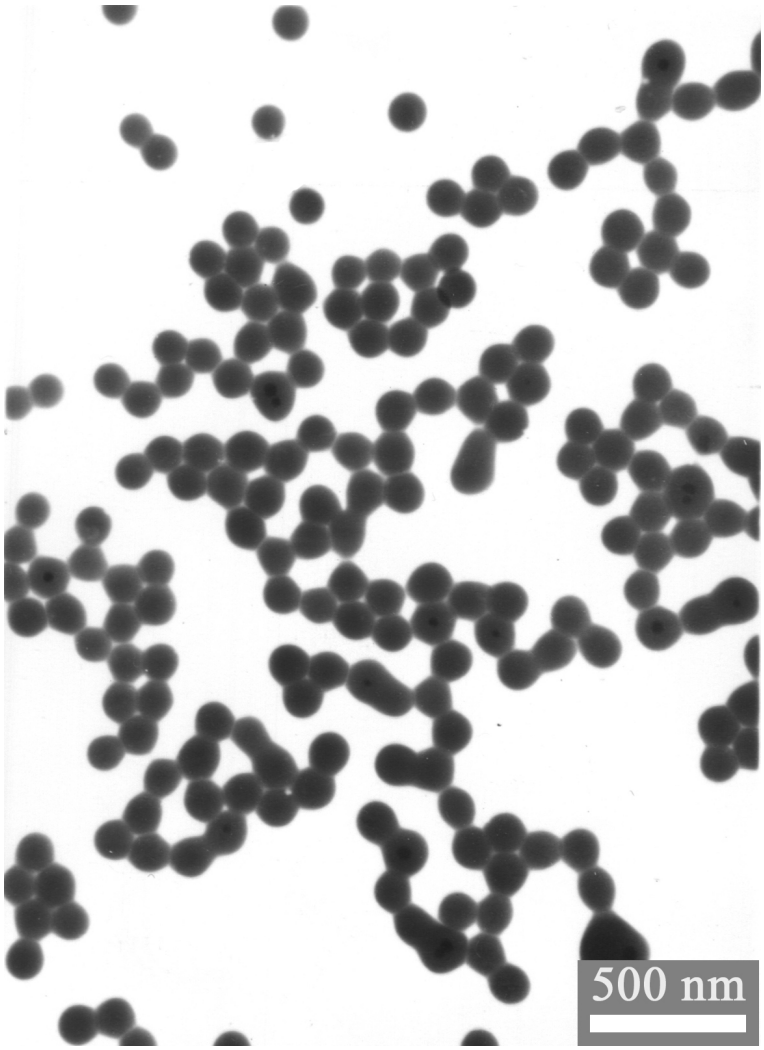

Figure S3. TEM image of the as-prepared Te nanoparticles and nanoparticle-joint quai-1D nanomaterials prepared in the presence of 0.09 g H_2TeO_3, 0.005 g PVP, 1 mL $N_2H_4 \cdot H_2O$ and 100 mL H_2O by using the visible-light assisted method.

S4 SEM image of the as-prepared Te nanobelts obtained in this visible-light assisted approach.

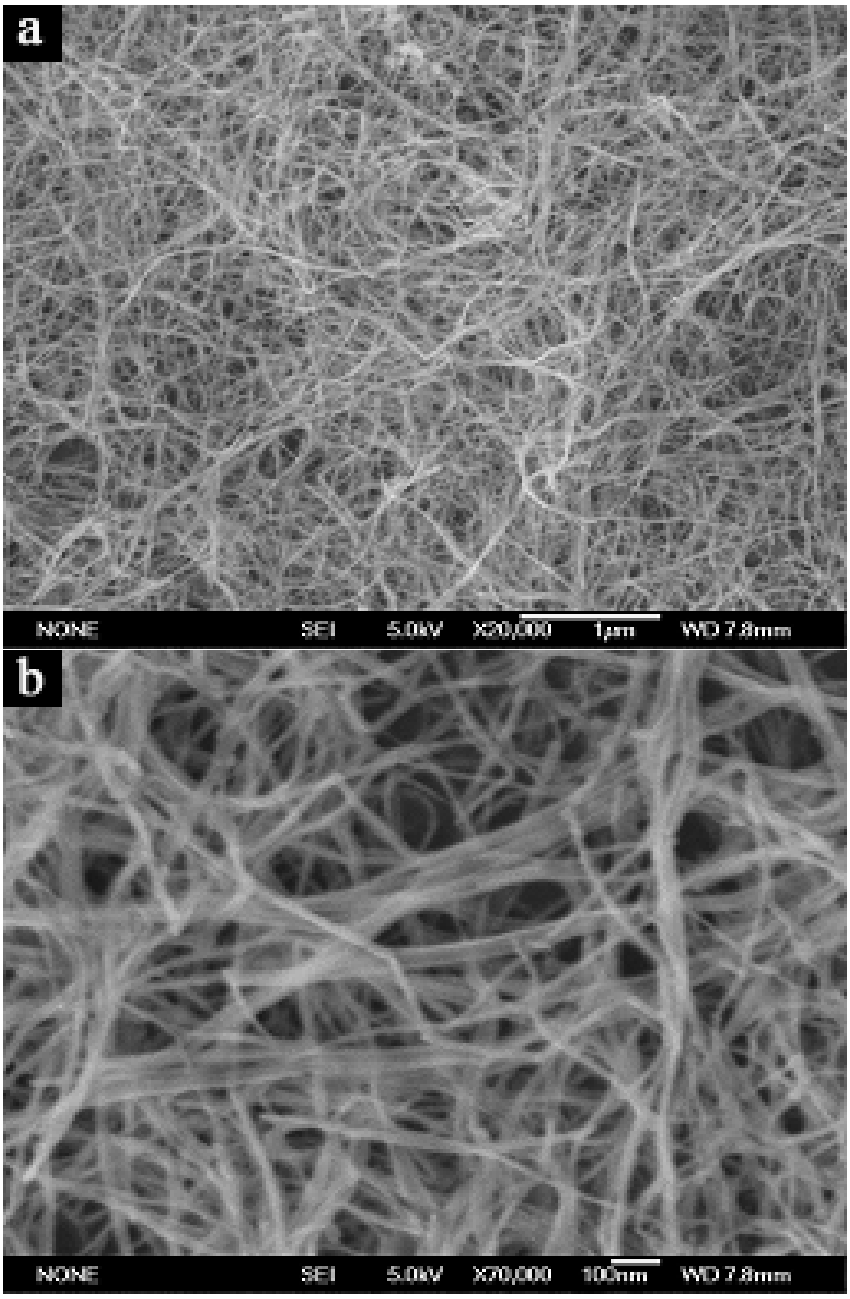

Figure S4. Low-magnification (a) and high-magnification (b) FESEM image of the as-prepared Te nanobelts using the visible-light assisted method, revealing the large-scale preparation of Te nanoribbons. The belt-like samples was prepared in the presence of in the presence of 0.09 g H_2TeO_3, 1.5 mL PVA (3 wt %), 1 mL $N_2H_4 \cdot H_2O$ and 100 mL H_2O

S5. TEM images and HRTEM image of the as-prepared Te nanorods and nanowires with a diameter of ca. 7.5 nm using photothermally assisted method.

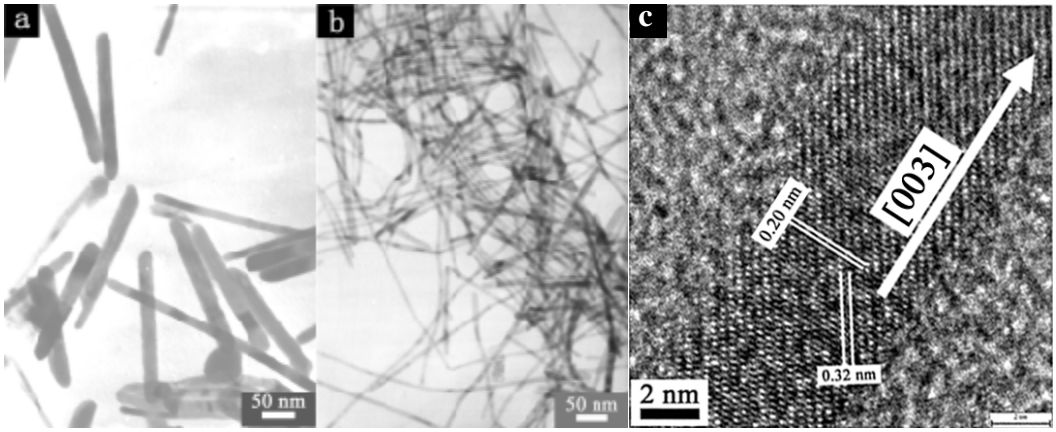

Figure 52. TEM images of two different Te products: a) Nanorods, prepared in the presence of 0.27 g H_2TeO_3, 0.05 g PVP, 100 mL H_2O, indicating that the Te nanorods can be also fabricated using this facile photothermal method; b, c) TEM (b) and HRTEM (c) images of Te nanowires with a diameter of about 7.5 nm, synthesized in the presence of 0.09 g H_2TeO_3, 0.05 g PVP, 2 mL 5M KOH and 78 mL H_2O. The HR-TEM image shows that the nanowires have the diameter of ca. 7.5 nm and a preferential growth direction along the *c*-axis of Te. The diameter of these Te nanowires is lower than that of the nanowires prepared without the addition of KOH (see Figure 2a,b, Figure 5 and Figure S1), showing that the diameter of the Te samples may be adjusted by the addition of alkali.

S6. SAED patterns and HRTEM images of as-prepared t-Te nanobelts prepared using phoththermally assisted method.

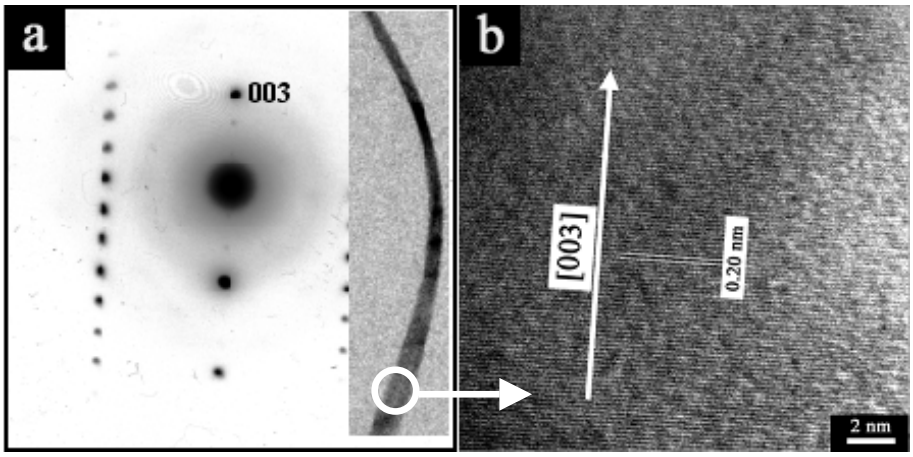

Figure S6. a) SAED patterns of one Te nanoribbon. The inset is associated with SAED pattern. b) Corresponding HRTEM image revealing the clear lattice of the nanoribbons. The fringe spacing of 0.20 nm observed in this image corresponds to the separation of the (003) lattice plane, indicating the preferential growth along the [001] direction.

S7. TEM images of as-prepared t-Te irregular nanoparticles prepared using the typical refluxing technique.

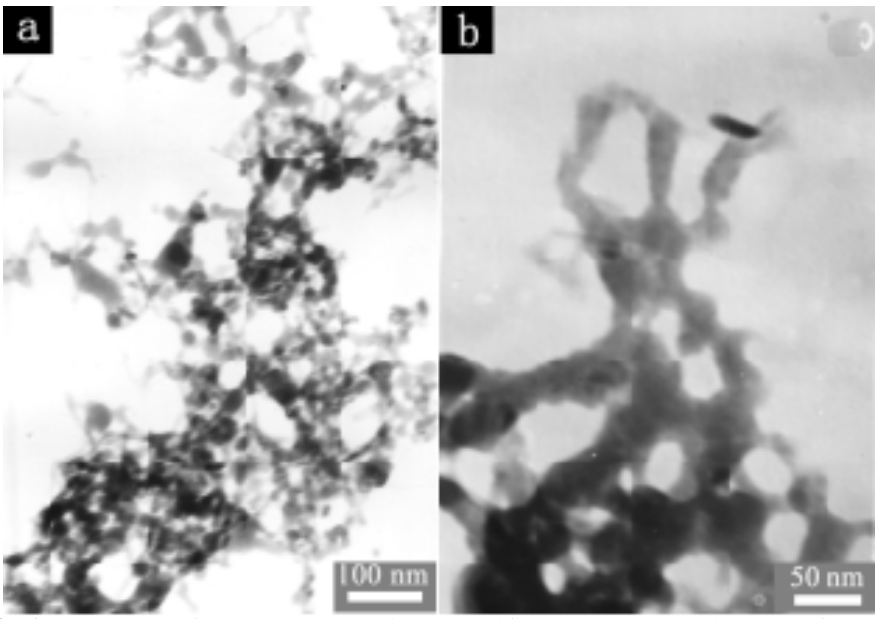

Figure S7-1. Low-magnification (a) and high magnification (b) TEM images of as-prepared irregular Te nanoparticles when the oil bath and refluxing solution controlled at ~100 ºC in the presence of 0.09 g H_2TeO_3, 0.05 g PVP, 100 mL H_2O. The associated SAED pattern (not shown here) indicates the amorphous nature. The shape is obviously different from that of the nanowires with high crystallinity (Figure 2a, Figure S1 and Figure 5), indicating that the light has an important role in the synthesis of Te nanomaterials. Owing to the fact that the solution-phase temperature was about 100 ºC when a lawn lamp of 500 W was adopted, the refluxing temperature was also controlled at ~ 100 ºC.

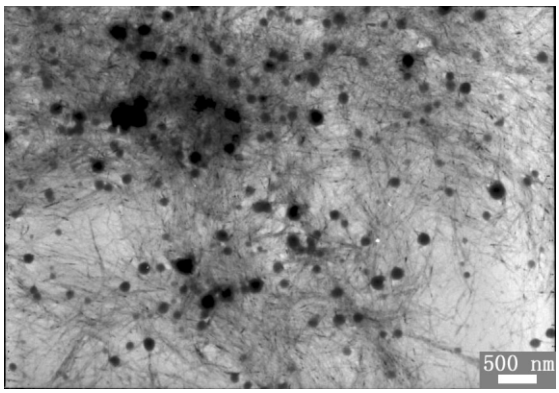

Figure S7-2. TEM image of as-prepared nanospheres and Te nanowires when the oil bath and refluxing temperatures are 150 ºC and 100, respectively. The samples are prepared in the presence of 0.09 g H_2TeO_3, 0.05 g PVP, 100 mL H_2O. From the TEM image, it can be seen that besides Te nanowires, there are still some nanoparticles in the final products. But all the as-prepared products obtained using the visible-light assisted method were nanowires, as revealed in TEM (Figure 2a) and SEM (Figure S 1) observations. This shows that the presence of light can conduce to the 1D nanowires, confirming the importantance of light in the photothermal method.

S8. Optical images of as-prepared t-Te products using different methods.

Figure S8. Optical images of the Te samples prepared in the presence of 0.09 g H_2TeO_3, 0.05 g PVP, 100 mL H_2O using different methods. a) Amorphous irregular Te nanoparticles (Figure S7) synthesized by using the refluxing technique. The samples were directly extracted form the final reaction solutions and took by digital camera without the flash lamp. b) Nanowires prepared using visible-light assisted method. The corresponding SEM and TEM images are shown in Figure S2-1 and Figure 2a, respectively. The samples were directly extracted form the final reaction solutions and took by digital camera without the flash lamp.

S9. Intermediates of the Tellurium nanowires collected at different stages in the photothermally-assisted method.

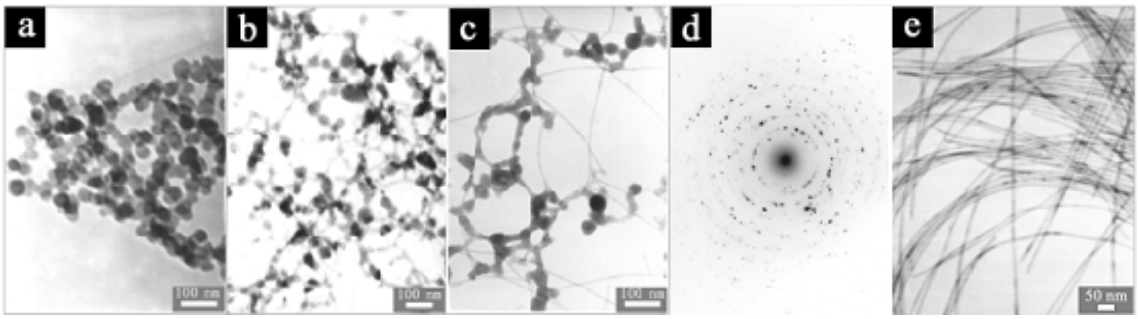

Figure S9-1. TEM images of intermediates collected in the formation process of Te nanowires with different times: a) 40 min, b) 80 min, c) 3h, e) 8h. These samples were prepared from 0.09 g H_2TeO_3, 0.05 g PVP and 100 mL H_2O. The Figure S9-1d is the SEAD pattern associated with the samples of Figure S9-1c.

To understand the growth mechanism of Te nanowires prepared by the photothermal method, TEM was used to characterize the intermediates collected at different reaction stages. Figure S9-1a shows the TEM image of spherical intermediates when the reaction time is 40 min. Further SAED study (not shown here) indicates the amorphous nature, suggesting that H_2TeO_3 was firstly reduced to amorphous Te particles (a-Te) by hydrazine hydrate ($N_2H_4 \cdot H_2O$). When the reaction mixture was irradiated under the illumination of the visible light for 80 min, the samples become nanoparticle-joint quasi-1D nanostructures, as shown Figure S9-1b. When the photothermal time was increased to 3h, the mixture of particle-joint nanochains and nanowires was observed (Figure S9c). The SAED pattern shown in the Figure S9-1d reveals that the intermediates are crystalline, suggesting the existence of triagonal tellurium (t-Te). This suggests that the particles-joint nanochains slowly developed into crystalline wire-like nanostructures with the increasing reaction time. The transformation of a-Te into t-Te, which is thought to be the Ostwald ripening process, has also been observed in the Se materials.(B. Gates, Y. D. Yin, Y. N. Xia, *J. Am. Chem. Soc.* **2000**, *122*, 12582; B. Mayers, Y. N. Xia, *J. Mater. Chem.* **2002**, *12*, 1875) In the following process, the spheres-joints structures completely transformed into triagonal nanowires with high crystallinity (Figure S9-1d and Figure 5). The transformation from a-Te to t-Te and the sphere-wire mechanism are very similar to that of Se nanowires. (B. Gates, B. Mayers, B. Cattle, Y. N. Xia, *Adv. Funct. Mater.* **2002**, *12*, 219; B. T. Mayers, K. Liu, D. Sunderland, Y. N. Xia, *Chem. Mater.* **2003**, *15*, 3852).

As for the growth mechanism of other Te 1D nanostructures under the photothermal-assisted approach, we believe that the a-Te firstly formed after lighting the lawn lamp, and then some a-Te spheres transformed into t-Te seeds because of the rather lower free energy of t-Te relative to a-Te. The amount of water-soluble polymers has a noticeable influence on the products' morphology, especially for the formation of the seeds. For example, when the amount of PVP was increased from 0.05 g to 0.15 g (the final Te products changed from nanowires to nanotubes), the cylindrical seeds were observed in the TEM image displayed in Figure S9-2, which has been considered to an important step for the concentration-depletion mechanism on the surface of the cylindrical seeds that Xia et al. proposed for Te nanotubes. (B. Mayers, Y. N. Xia, *Adv. Mater.* **2002**, *14*, 279) Note that the explanation for the growth process of selenium nanostructures/submicrostructures under the photothermal-assisted approach are rough, and more systematic work need to be done to get a better knowledge on the formation mechanism, which is now underway in our group.

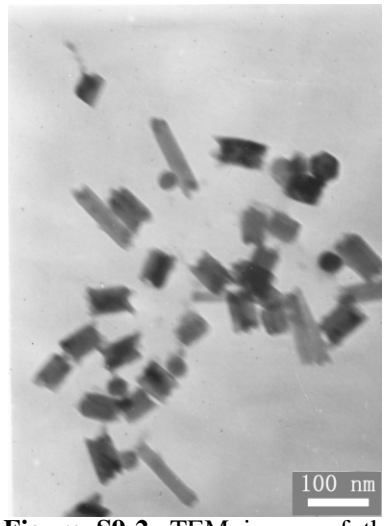

Figure S9-2. TEM image of the intermediates appearing in the formation of Te nanotubes by this photothermal assisted approach.

S10. HRTEM images of the Te-Pt nanochains with a composition ratio of 45:55 (Te : Pt).

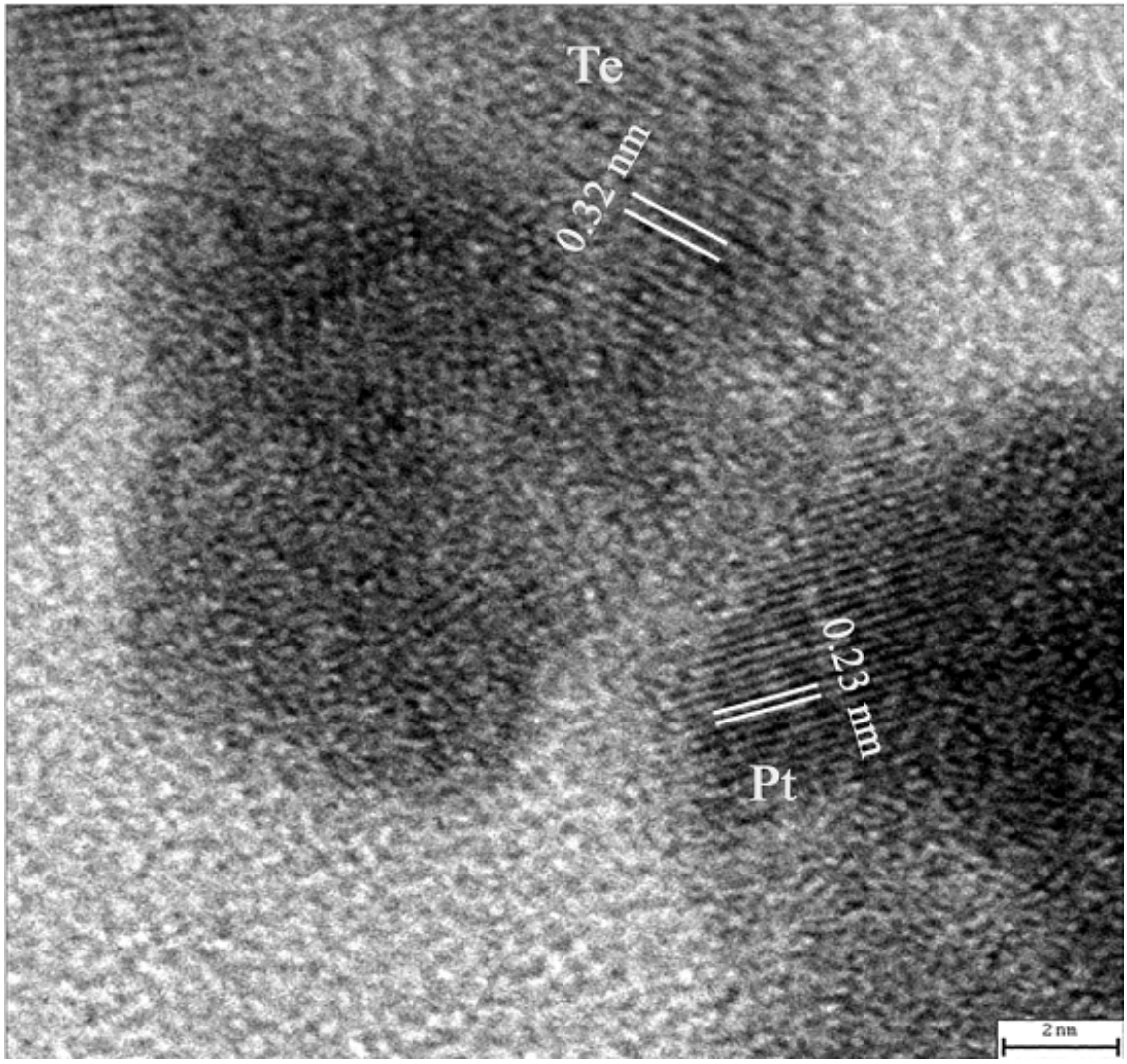

Figure S10-1. A HRTEM image of the Pt-Te nanochains obtained through the room temperature galvanic replacement reaction between Te nanowires and H_2PtCl_6. The samples were prepared by galvanic replacement reaction between the Te nanowires (4 mL water-containing solution and H_2PtCl_6 (0.015 M, 1.25 mL). The clearly observed HRTEM spacing of 0.32 nm and 0.23 nm match well with the separations of Te (101) and Pt (111) planes, respectively.

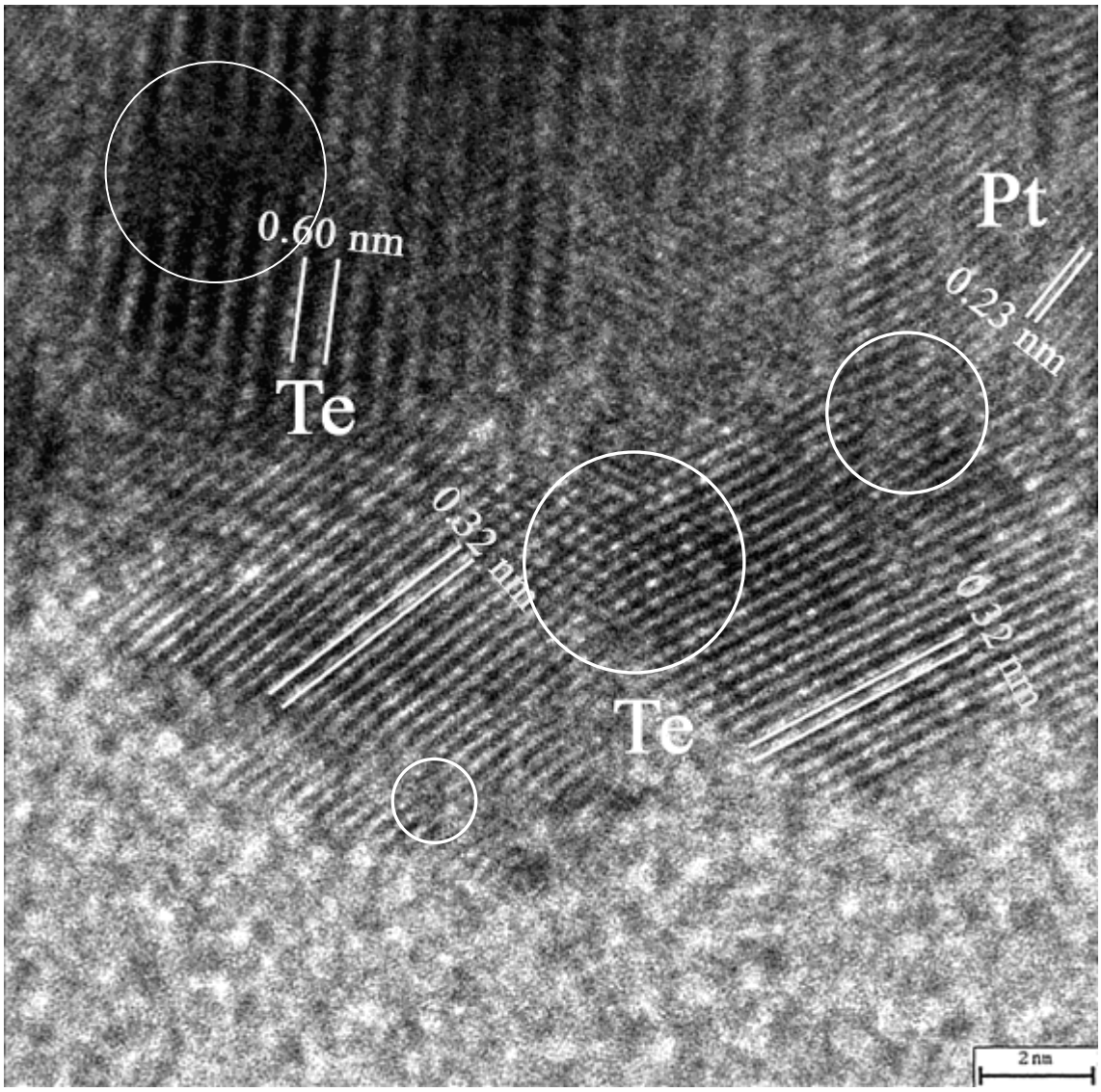

Figure S10-2. Another HRTEM image of the Pt-Te nanochains, suggesting the polycrystalline structure of the samples. The samples were prepared by galvanic replacement reaction between the Te nanowires (4 mL water-containing solution and H_2PtCl_6 (0.015 M, 1.25 mL). The circles indicate the positions that there exist defects or dislocations in the as-prepared Pt-Te nanochains.

S11. TEM images and EDAX spectrum of the obtained Te-Pt nanochains with the composition ratio of 53:47 (Te:Pt).

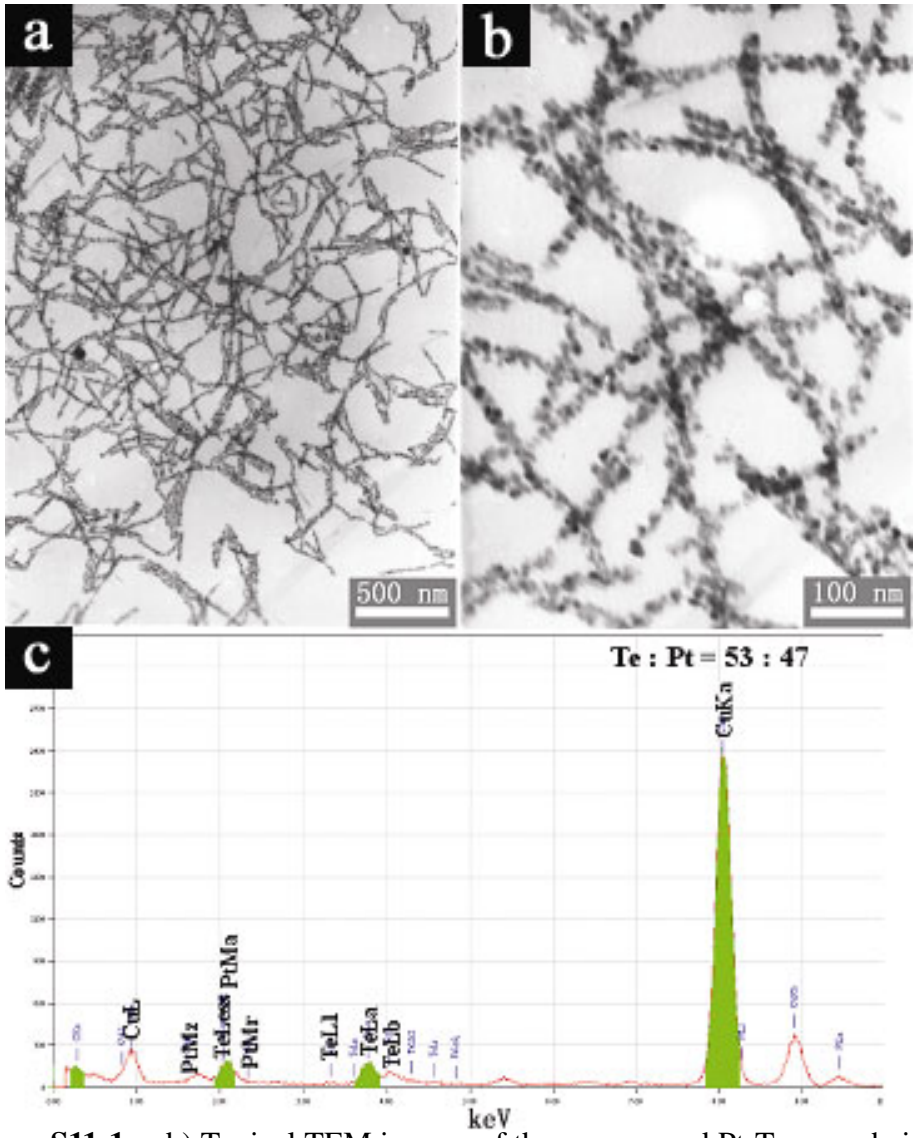

Figure S11-1. a-b) Typical TEM images of the as-prepared Pt-Te nanochains at different magnifications. d) EDAX spectra of the as-prepared nanochains, revealing the composition of Te and Pt with a ratio of ca. 53:47. The Pt composition is lower than that shown in Figure 3a,b, indicating that the relative composition of Pt and Te can controlled by changing the amount of the reacting agents. The samples were prepared by galvanic replacement reaction between the Te nanowires (4 mL water-containing solution and H_2PtCl_6 (0.015 M, 1 mL). Note that the ratio of Te to Pt in the final products is slightly different from the stoichiometric proportion of the reacting agents, which may be attributed to the consumption of the Te nanowires in reducing H_2PtCl_6 to Pt and the loss in the pretreatment.

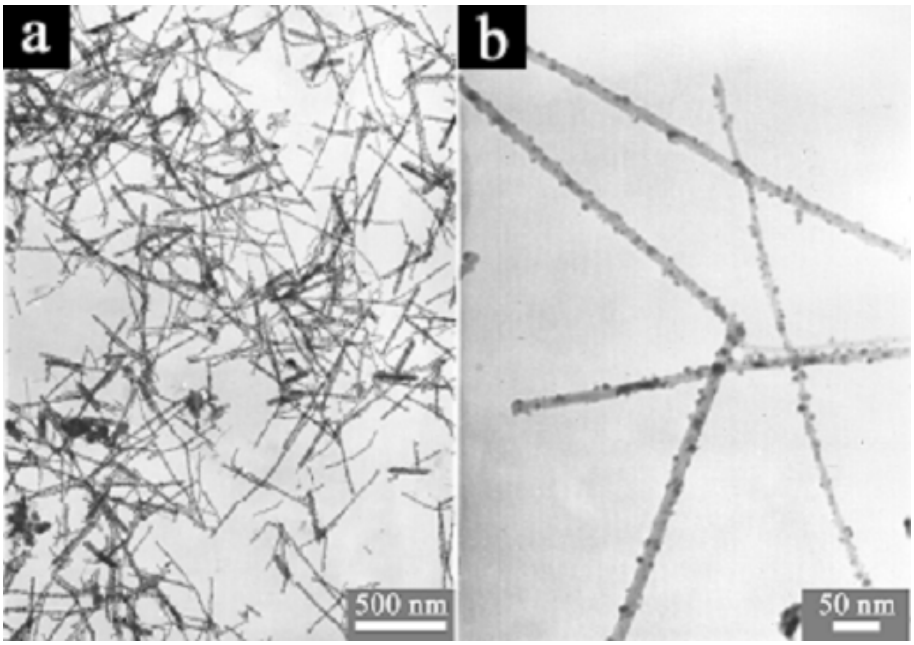

Figure S11-2. Low-magnification (a) and high-magnification (b) TEM images of the as-prepared Pt-Te nanochains prepared by galvanic replacement reaction between the Te nanowires (4 mL water-containing solution) and H_2PtCl_6 (0.015 M, 0.5 mL). From the high-magnification TEM image (Figure S11-2), fewer Pt nanoparticles was attached on the surface of the Te nanowires. The coverage of Pt nanoparticles on the Te wires are obviously lower than that of the Pt-Te nanochains with different ratios of 53:47 and 45:55 (Te:Pt), suggesting that the ratio of Te to Pt is higher than the Pt-Te composite nanochains shown in Figure 6a and Figure S11-1b and confirming that the relative composition of Pt and Te can be controlled by modulating the amount of the reacting agents.

S12. HRTEM image of the as-prepared Te-Pt@carbon-rich nanocables.

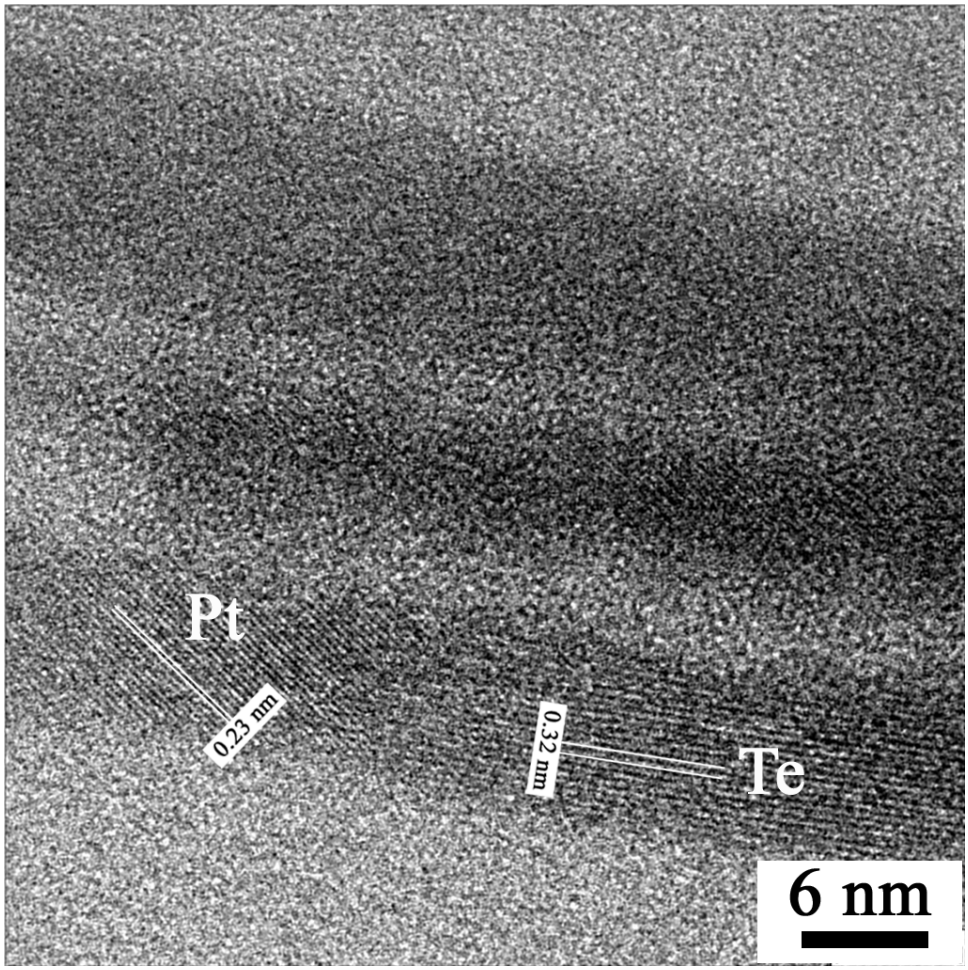

Figure S12. A Typical HRTEM image of the Te-Pt@carbon-rich nanocables obtained through the room temperature galvanic replacement reaction between Te-Pt nanochains and H_2PtCl_6. The samples were prepared by the hydrothermal reaction of Te-Pt nanochains and glucose. The clearly observed HRTEM spacing of 0.32 nm and 0.23 nm match well with the separations of Te (101) and Pt (111) planes, respectively, suggesting that the core in the Te-Pt@carbon-rich nanocables consist of Pt and Te.